Hindawi
Advances in Materials Science and Engineering
Volume 2022, Article ID 5468264, 11 pages
https://doi.org/10.1155/2022/5468264

Research Article

Moisture Stability of Hard Sandstone Asphalt Mixture Based on APT with MMLS3

Zhang Ermao,[1] Yang Liming,[2] and Yang Datian [3]

[1]*Nanning Expressway Construction & Development Co., Ltd., Nanning 530023, China*
[2]*Guangxi Communication Design Group Co., Ltd, Nanning 530029, China*
[3]*College of Civil Engnieering, Chongqing Jiaotong University, Chongqing 400074, China*

Correspondence should be addressed to Yang Datian; tywoyangda@126.com

Received 11 April 2022; Revised 15 June 2022; Accepted 16 June 2022; Published 30 June 2022

Academic Editor: Chunli Wu

Copyright © 2022 Zhang Ermao et al. This is an open access article distributed under the Creative Commons Attribution License, which permits unrestricted use, distribution, and reproduction in any medium, provided the original work is properly cited.

To evaluate the moisture stability of a hard sandstone asphalt mixture, a testing section of a hard sandstone asphalt mixture was prepared in the laboratory. The accelerated pavement testing (APT) with the one-third-scale model mobile load simulator (MMLS3) was conducted in this testing section under temperature and water-coupled conditions. As the APT number increased, the elastic modulus of the hard sandstone asphalt mixture pavement gradually decreased. The average elastic modulus was 22.99 GPa after 160000 APT cycles. The bulk specific density of the sample rolled by the MMLS3 increased, and the residual indirect tensile strength ratio was 88.7%. Therefore, the hard sandstone asphalt mixture had good resistance to moisture damage, and hard sandstone aggregates can be used in a hot mix of asphalt.

1. Introduction

Moisture damage is one of the diseases of asphalt mixture pavement [1]. The main external cause of moisture damage in asphalt pavement is the coupled effect of water, temperature, and vehicle loads. The main internal causes of water damage in asphalt pavement are the properties of the aggregate and asphalt [2]. High temperatures reduce the asphalt viscosity, water erodes the asphalt film on the aggregates, and repeated loads accelerate the moisture damage of asphalt mixtures.

The indirect tensile strength ratio is used to evaluate the moisture stability of asphalt mixtures in the standard method [3, 4]. Based on a certain sinusoidal waveform [5–9], water moves in the core in a compacted asphalt mixture sample, which simulates hydraulic scouring. After this moisture conditioning, the indirect tensile strength or dynamic modulus of the asphalt mixture sample is measured [10].

An immersion rutting test is a procedure in which a rolling tire compacts asphalt mixture specimens in the presence of water and measures the rutting depth after each rolling cycle. The rutting depth curves versus rolling cycles are then processed to determine the asphalt mixture's moisture stability. For this immersion rutting test, the Hamburg wheel-track test (HWTT) and an asphalt pavement analyzer (APA) are used to evaluate the moisture susceptibility of asphalt mixtures [11–14]. Twagira and Jenkins [15] used a one-third-scale model mobile load simulator (MMLS3) and tensile strength retention to evaluate the moisture damage and reveal the performances of bitumen stabilized materials.

The aggregate used in the hot mix asphalt is a nonrenewable resource, especially for individual aggregate types that are gradually becoming scarce, such as basalt aggregate and diabase aggregate. To solve the shortage problem of aggregate in asphalt mixtures, hard sandstone aggregate is being used in asphalt mixture pavement. Ouyang et al. [16] used sandstone aggregate to study the highway performances of sandstone asphalt mixtures. Metcalf and Goetz [17] found that sandstone as an aggregate type can be satisfactorily used in asphalt pavement. Zhang and Li [18] used sandstone aggregate to produce sandstone concrete as the road base.

In this study, hard sandstone aggregate from an aggregate plant in Guangxi was used. To examine the moisture stability of the hard sandstone asphalt mixture, a testing section of the hard sandstone asphalt mixture pavement with a length of 4.2 m, a width of 1.4 m, and a thickness of 0.04 m was paved in the laboratory. Then, accelerated pavement testing (APT) with the MMLS3 under hot-water conditions was performed on the hard sandstone asphalt mixture pavement. The elastic modulus of the asphalt mixture pavement was measured with a portable seismic property analyzer (PSPA) after the APT. Finally, some core samples at the wheel and nonwheel track locations were drilled, and their indirect tensile strengths and bulk specific densities were measured. Then, their indirect tensile strength ratios were computed to evaluate their moisture stability. The materials and corresponding test methods used in this study are summarized as a flow chart, as shown in Figure 1.

2. Materials

2.1. Coarse Aggregate. In this study, the coarse aggregate was a type of hard sandstone aggregate that has been rarely used in asphalt mixtures. Its properties were measured by the Test Methods of Aggregate for Highway Engineering (JTG E42-2005) [19], as shown in Table 1.

2.2. Fine Aggregate. The fine aggregate was a limestone manufactured sand, whose properties are shown in Table 2.

2.3. Filler. The filler was a limestone grinding powder, whose properties are shown in Table 3.

2.4. Asphalt. Styrene-butadiene-styrene (SBS) modified asphalt was used, whose properties are shown in Table 4.

3. Aggregate Gradation and Optimal Asphalt Aggregate Ratio

In this paper, the optimal asphalt aggregate ratio was determined by the Marshall mix design method [20].

According to the Technical Specifications for Construction of Highway Asphalt Pavement (JTG F40-2004) [20], for hot areas in the summer with heavy traffic, the air void content (AV) of an AC-13C asphalt mixture ranges from 4% to 6%.

In this paper, the coarse aggregate with three size ranges (3–5 mm, 5–10 mm, and 10–15 mm) was used. The coarse aggregate of 3–5 mm was a limestone aggregate. Through aggregate sieve analysis and the specification requirements, the aggregate gradation was optimized as shown in Table 5 and Figure 2. Hence, the combined gradation is composed of 5% filler, 29% fine aggregate, 16% coarse aggregate of 3–5 mm, 26% coarse aggregate of 5–10 mm, and 24% coarse aggregate of 10–15 mm, whose percentages are the ratio of the mass of various aggregates to the mass of blended aggregates.

The bulk specific density, Marshall stability (MS), flow value (FL), air void content (AV), voids in the mineral aggregate (VMA), and voids filled with asphalt (VFA) were determined and are shown in Table 6 and Figure 3. In Figure 3, the horizontal axis corresponds to the asphalt aggregate ratio.

First, from Figure 3, the following points were determined:

(a) asphalt aggregate ratio, a_1, at the maximum bulk specific density

(b) asphalt aggregate ratio, a_2, at the maximum MS

(c) asphalt aggregate ratio, a_3, at the midpoint of the specified AV range (4%–6%)

(d) The asphalt aggregate ratio, a_4, at the midpoint of the specified VFA range (65%–75%)

Second, the average of the four asphalt aggregate ratios was computed, as follows:

$$\mathrm{OAC}_1 = \frac{(a_1 + a_2 + a_3 + a_4)}{4} = \frac{(4.7\% + 4.5\% + 5.0\% + 5.1\%)}{4} = 4.83\%. \quad (1)$$

Third, the range of the asphalt aggregate ratio, $C_{\min}$–$C_{\max}$, was determined, based on the Technical Specifications for Construction of Highway Asphalt Pavement (JTG F40-2004) [20] (excluding VMA). The average of the minimum and maximum values were computed, as follows:

$$\mathrm{OAC}_2 = \frac{(\mathrm{OAC}_{\min} + \mathrm{OAC}_{\max})}{2} = \frac{(3.8\% + 5.0\%)}{2} = 4.40\%. \quad (2)$$

Finally, the average of C_1 and C_2 were calculated, as follows:

$$\mathrm{OAC} = \frac{(\mathrm{OAC}_1 + \mathrm{OAC}_2)}{2} = \frac{(4.83\% + 4.40\%)}{2} = 4.6\%. \quad (3)$$

The optimal asphalt aggregate ratio was 4.6%.

4. Construction of Hard Sandstone Asphalt Mixture Pavement

To study the moisture stability of the hard sandstone asphalt mixture, a pavement sample of the hard sandstone asphalt mixture was constructed in the laboratory. This hard sandstone asphalt mixture pavement had a thickness of 0.04 m, length of 4.2 m, and width of 1.4 m. The construction procedure of the pavement sample is shown in Figure 4.

In the laboratory, workers removed the old asphalt mixture layer, then sprayed a seal coat, and finally, sprinkled the hot asphalt as the binder on the base. Because the mixing pot used in the laboratory only mixed 30 L of asphalt mixture at a time, about 500 kg of the hard sandstone asphalt mixture was mixed several times. The asphalt mixtures mixed each time were packed in a white iron bucket, which were then stored in an oven at 180°C, as shown in Figure 5.

Based on previous construction experience for AC-13C, the loose paving coefficient for AC-13C was 1.2. The hard

Figure 1: Flow chart of study materials and corresponding test methods.

Table 1: Properties of coarse aggregate.

Properties		Unit	Requirements	Results
Crushing value		%	≤26	23.4
Los Angeles abrasion		%	≤28	25.0
Bulk relative density	5–10 mm	—	≥2.60	2.715
	10–15 mm			2.714
Water absorption	5–10 mm	%	≤2.0	0.45
	10–15 mm			0.43
Flat and elongated particles (%)	>9.5	%	≤12	11.1
	<9.5		≤18	12.8
Washing method <0.075 mm		%	<1	0.9
Durability/soundness		%	≤12	6

sandstone asphalt mixtures were placed on the binding layer, as shown in Figure 6. After the hard sandstone asphalt mixtures were placed, about a 5-ton road roller-compacted them to a 40-mm thickness, as shown in Figure 7.

5. Accelerated Pavement Testing

5.1. One-Third Scale MMLS3. APT refers to "the controlled application of a prototype wheel loading, at or above the appropriate legal load limit to a prototype or actual, layered, structural pavement system to determine pavement response and performance under a controlled, accelerated accumulation of damage in a compressed time period. The acceleration of damage is achieved by means of increased repetitions, modified loading conditions, imposed climatic conditions, the use of thinner pavements with a decreased structural capacity and thus shorter design lives, or a combination of these factors. Full-scale construction by

Table 2: Properties of fine aggregate.

Properties	Unit	Technical requirements	Results
Apparent relative density	—	≥2.50	2.62
Durability/soundness	%	≤12	0.9
Mud content	%	≤3	1.8
Methylene blue value	g/kg	≤25	16
Angularity	s	≥30	45

Table 3: Technical properties of filler.

Properties		Unit	Technical requirements	Results
Apparent density		g/cm^3	≥2.50	2.679
Water content		%	≤1	0.3
Hydrophilic coefficient		—	<1	0.75
Particle size	<0.6 mm	%	100	100
	<0.15 mm	%	90–100	98.8
	<0.075 mm	%	75–100	87.4

Table 4: Technical properties of SBS modified asphalt.

Properties		Unit	Technical requirements	Results
Penetration depth at 25°C, 100 g, 5 s		0.1 mm	40–60	50
Penetration index		—	≥0	1.152
Softening point (ring and ball method)		°C	≥60	85.0
Ductility at 5 cm/min, 5°C		cm	≥20	39
Specific relative density at 15°C		—	—	1.060
Kinematic viscosity at 135°C		Pa·s	≤3	1.2
Flash point temperature		°C	≥230	303
Solubility in trichloroethylene		%	≥99	99.54
Elasticity recovery at 25°C		%	≥75	81
Rolling thin-film oven test at 163°C	Weight change	%	±1.0	−0.105
	Retained penetration	%	≥65	67
	Ductility at 5°C	cm	≥15	19

Table 5: Combined gradation.

Sieve size (mm)	Mass percentage passing through the sieve (%)									
Gradation	0.075	0.15	0.3	0.6	1.18	2.36	4.75	9.5	13.2	16
Upper limit of gradation	8	15	20	28	38	50	68	85	100	100
Lower limit of gradation	4	5	7	10	15	24	38	68	90	100
Middle limit of gradation	6	10	13.5	19	26.5	37	53	76.5	95	100
Combined gradation	5	8	11	16	24	34	50	76	95	100

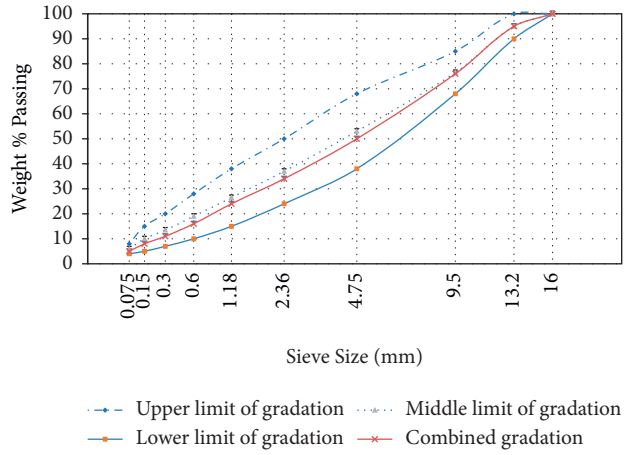

Figure 2: Aggregate gradation curve.

Table 6: Marshall testing results.

Asphalt aggregate ratio (%)	Bulk specific density	AV (%)	VMA (%)	VFA (%)	MS (kN)	FL (mm)
3.5	2.380	6.42	16.29	60.58	21.71	2.01
4.0	2.398	5.70	16.05	64.47	23.93	2.97
4.5	2.413	5.28	15.97	66.94	24.33	3.57
5.0	2.412	5.00	16.54	69.77	22.91	4.09
5.5	2.382	4.76	16.84	71.73	19.94	4.56

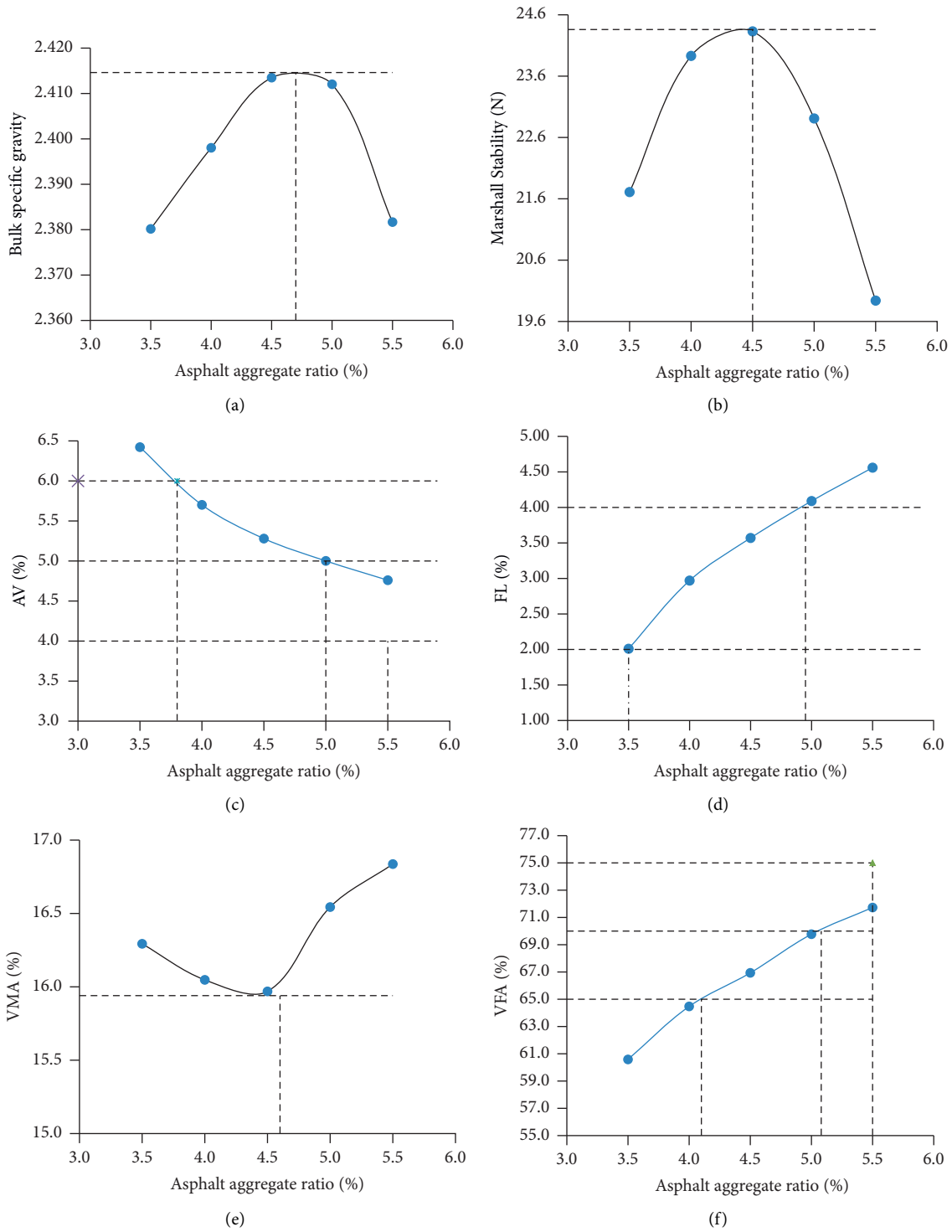

Figure 3: Design plots for Marshall mix design.

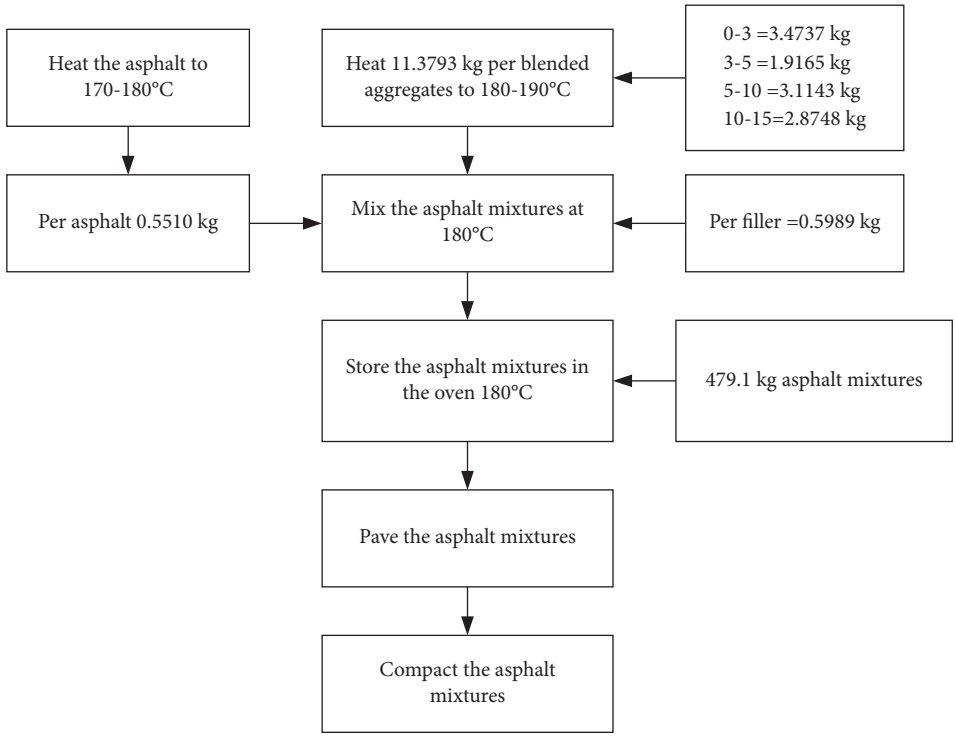

Figure 4: Construction flow chart for the hard sandstone asphalt mixture testing section.

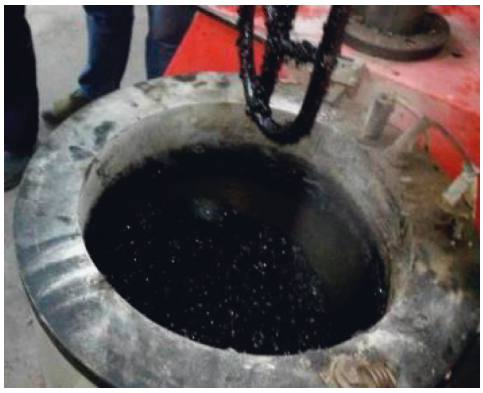

Figure 5: Mixing the hard sandstone asphalt mixture.

Figure 6: Paving the hard sandstone asphalt mixture.

conventional plant and processes is necessary so that real-world conditions are modeled" [21].

The MMLS3 [22] can apply 7200 wheel loads per hour. The maximum wheel load was 2.7 kN (2.9 kN for short periods) on the 300-mm-diameter pneumatic tire wheels. The maximum tire pressure was 700 kPa (800 kPa for short periods). The MMLS3 included an electronic wheel load calibration unit, one spare load wheel, eight spare guide wheels, spare drive belts, a tool kit, and a canvas cover, as shown in Figure 8.

Figure 7: Compacting the hard sandstone asphalt mixture.

5.2. Wet Heater System. The water heater unit was used to circulate and heat the water to be applied onto the material to be tested. It can be used in conjunction with a set of spray nozzles to spray hot water onto the pavement in the field or a slab in the laboratory while it is being trafficked by the

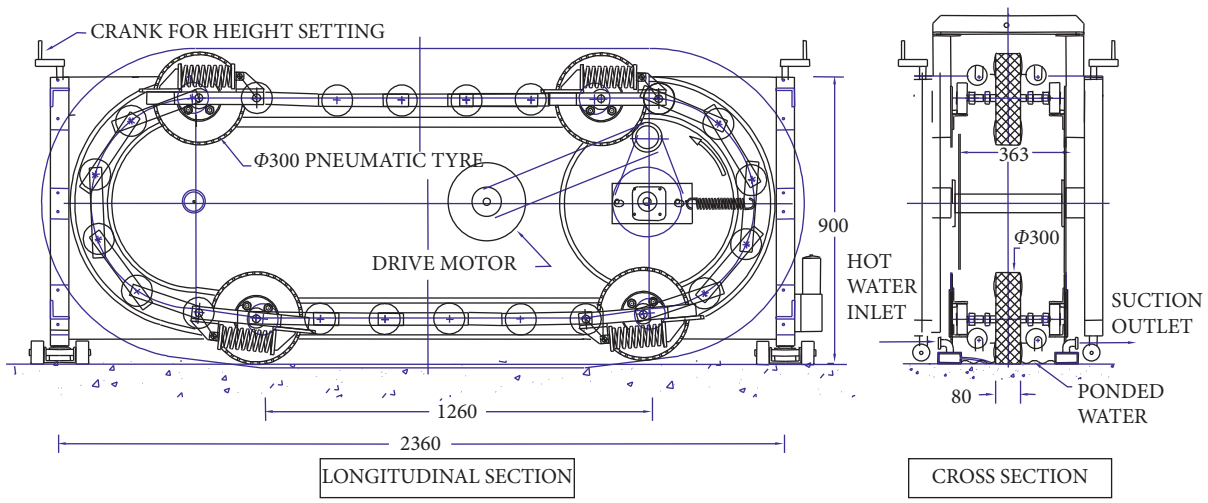

Figure 8: Schematic diagram of MMLS3.

Figure 9: MMLS3 and water heater unit.

MMLS3. In this study, the hard sandstone asphalt mixture pavement was mainly heated by spraying hot water at 80°C, which resulted in hot and humid environmental conditions, as shown in Figure 9.

5.3. Testing Locations. The testing pavement was divided into four segments to measure their elastic moduli separately, as shown in Figure 10.

5.4. PSPA. The elastic moduli of the hard sandstone asphalt mixture pavement were measured by the seismic wave method, namely using a PSPA [23], as shown in Figures 11 and 12. Because the hard sandstone asphalt mixture pavement was heated by hot water, the elastic moduli measured by the PSPA were transformed into the elastic moduli at 25°C using the following equation [24]:

$$E_{25} = \frac{E_t}{1.35 - 0.01404t}, \quad (4)$$

where E_{25} and E_t are the modulus at 25°C and temperature t (°C), respectively.

5.5. Experimental Plan. The numbers of passes during the APT were 0, 5000, 10000, 20000, 40000, 80000, and 160000. After the APT, the elastic moduli of four testing segments

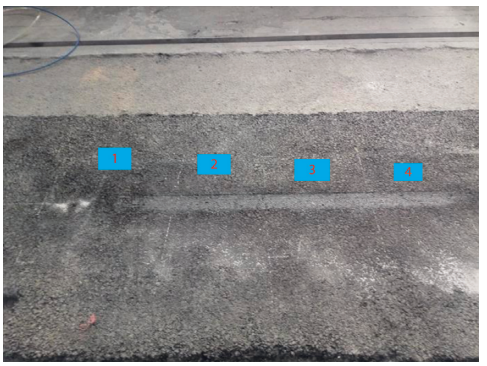

Figure 10: Measurement locations for PSPA.

Figure 11: PSPA.

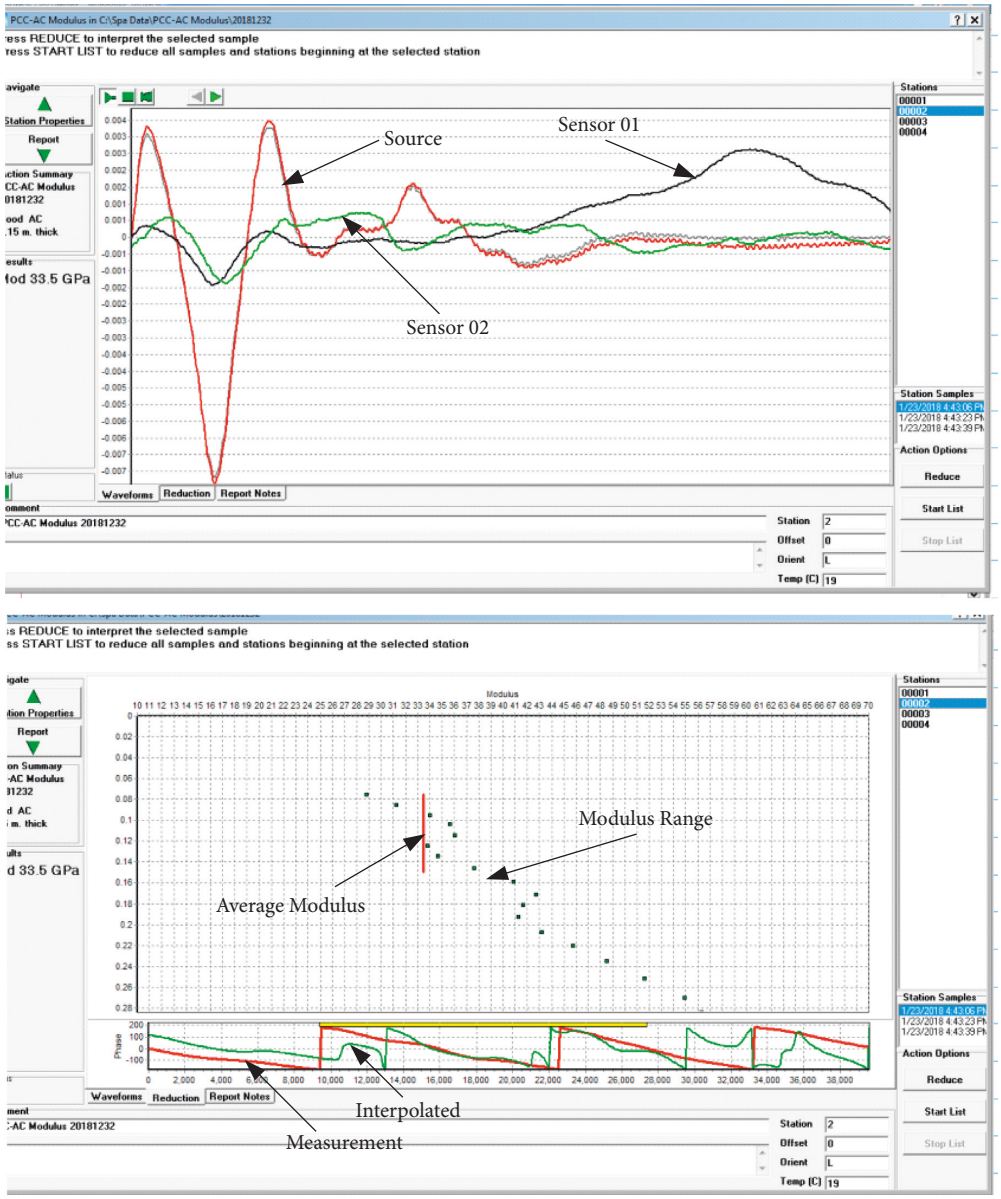

Figure 12: PSPA time records and dispersion curves.

were measured. Finally, the core specimens were drilled at the wheel track and nonwheel track. Their bulk specific density and the indirect tensile strength were measured in the laboratory.

6. Results and Discussion

6.1. Elastic Modulus of Hard Sandstone Asphalt Mixture. As shown in Figure 10, there were two segments completely rolled by the MMLS3. The first and fourth segments were only partially rolled. Hence, the elastic moduli of the second and third segments are discussed here. The elastic moduli of the hard sandstone asphalt mixture pavement segments are shown in Table 7.

According to Grubbs' statistical method [25], the elastic modulus of 117.13 GPa in Segment 2 was an outlier. This outlier was excluded, and the elastic modulus of the hard sandstone asphalt mixture pavement ranged from 11.13 to 57.1 GPa and decreased to 22.60–23.37 GPa after 160000 loading cycles, as shown in Figure 13.

From Figure 13, as the number of loading cycles increased, the elastic moduli gradually decreased.

6.2. Bulk Specific Density and Indirect Tensile Strength. After the hard sandstone asphalt mixture pavement was rolled repeatedly by the MMLS3, some core specimens were drilled from the wheel track of the MMLS3, as shown in Figure 13. In addition, other core specimens were drilled from sites that were not rolled by the MMLS3, as shown in Figure 14.

The bulk specific densities and the indirect tensile strengths of these core specimens were measured in the laboratory. These results are shown in Table 8. The bulk

Table 7: Elastic moduli of the hard sandstone asphalt mixture pavement segments.

APT cycles	0	5000	10000	20000	40000	80000	160000
Segment 2	117.13	57.10	30.4	21.40	35.37	25.50	22.60
Segment 3	44.10	14.53	58.95	11.13	30.67	25.87	23.37

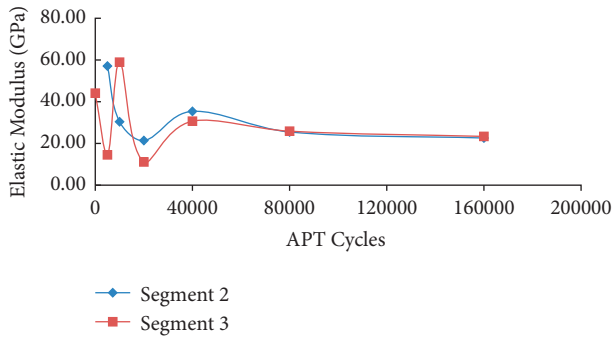

Figure 13: Relationships between the elastic moduli and the number of APT cycles for two segments.

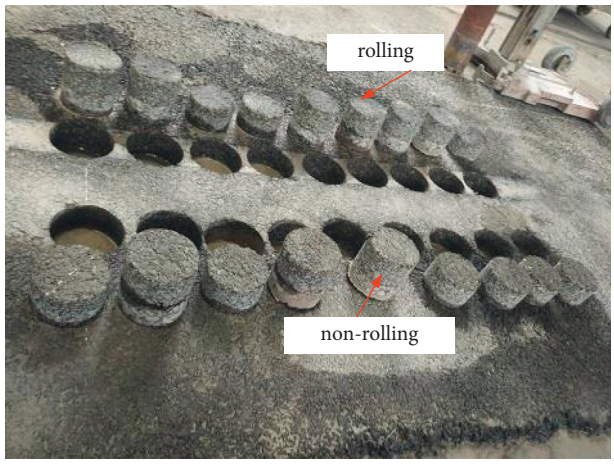

Figure 14: Core specimens.

Table 8: Bulk specific densities and indirect tensile strengths of two types of core specimens.

Number	Bulk specific density		Indirect tensile strength (MPa)	
	Rolled specimens	Nonrolled specimens	Rolled specimens	Nonrolled specimens
1	2.369	2.341	1.307	1.417
2	2.356	2.335	1.230	1.297
3	2.351	2.326	1.243	1.408
4	2.334	2.337	1.126	1.403
5	2.342	2.324	1.179	1.283
6	2.349	2.334	1.108	1.399
7	2.364	2.333	1.319	1.394
8	2.372	2.329	1.249	1.501
9	2.364	2.324	1.427	1.518
Average value	2.356	2.331	1.243	1.402

Table 9: t-test for the bulk specific densities of two types of core specimens.

t-test: paired two sample for means		
Sample	Sample 1	Sample 2
Mean	2.356	2.3314
Variance	0.0001633	3.628×10^{-05}
Observations	9	9
Pearson correlation coefficient	0.04765	
Hypothesized mean difference	0	
df	8	
t Stat	5.242	
$P(T\le t)$ one-tailed	0.0003909	
t critical one-tailed	1.860	
$P(T\le t)$ two-tailed	0.0007818	
t critical two-tailed	2.306	

Table 10: t-test for the indirect tensile strengths of two types of core specimens.

t-test: paired two sample for means		
Sample	Sample 1	Sample 2
Mean	1.243	1.402
Variance	0.01004	6.112×10^{-03}
Observations	9	9
Pearson correlation coefficient	0.5053	
Hypothesized mean difference	0	
df	8	
t Stat	−5.263	
$P(T\le t)$ one-tailed	0.0003807	
t critical one-tailed	1.860	
$P(T\le t)$ two-tailed	0.0007614	
t critical two-tailed	2.306	

specific density increased and the indirect tensile strength decreased after the APT. The cause of the bulk specific density increase was that the air void content was smaller in the hard sandstone asphalt mixture pavement rolled repeatedly by the MMLS3. Under conditions with water, temperature, and load coupling, microdamage could occur in the hard sandstone asphalt mixture, which made the indirect tensile strength smaller. However, the residual indirect strength ratio was still 88.7%, which fully meets the technical requirements of the moisture stability of hot mix asphalt [17].

To verify the significance of the effect of the wet-heated APT with the MMLS3 on the bulk density and the indirect tensile strength, the bulk specific density and the indirect tensile strengths of the two types of core samples were analyzed by the t-test method, as shown in Tables 9 and 10. According to the Pearson correlation coefficient of 0.04764 shown in Table 9, the linear correlation between the two types of samples was good. The one-tailed and two-tailed $P(T\le t)$ values were both smaller than the significance level of 0.05, which verified that there was a significant difference between them. Hence, the APT with the MMLS3 further compacted the hard sandstone asphalt mixture.

According to the Pearson correlation coefficient of 0.5052 shown in Table 10, the linear correlation between the two types of samples was a subpositive correlation. The one-

tailed and two-tailed $P(T \leq t)$ values were both smaller than the significance level of 0.05, which verified that there was a significant difference between them. Hence, under conditions with water, temperature, and load coupling, the APT with the MMLS3 could accelerate the damage to the hard sandstone asphalt mixture.

7. Conclusion

In this study, the moisture damage of a hard sandstone asphalt mixture was investigated using APT with an MMLS3. The elastic modulus of the hard sandstone asphalt mixture pavement as well as the bulk specific densities and indirect strengths of the specimens drilled from rolled and nonrolled sites were analyzed by the *t*-test method. The elastic modulus initially increased and then gradually decreased. The average elastic modulus was 22.99 GPa after 160000 APT cycles.

It was also found that the bulk specific density increased and the indirect tensile strength decreased after the APT with the MMLS3. The bulk specific density increased by 1.1%. The indirect tensile strength ratio of the two types of core samples was 88.7%. Based on a paired *t*-test, the bulk specific densities and indirect tensile strengths of the two types of core samples were significantly different at the significance level of 0.05. Hence, the hard sandstone asphalt mixture had a good ability to resist moisture damage.

In the future, it would be necessary to further track the changes in the highway performance of hard sandstone asphalt mixture pavement in the field and further carry out fatigue tests of hard sandstone asphalt mixtures. In addition, the differences between the hard sandstone aggregate, limestone aggregate, basalt aggregate, and diabase aggregate will be investigated. These results will be presented in successive publications.

Data Availability

The data in the manuscript were obtained by experiments, and the data were effectively collected and correctly presented. The data used to support the findings of this study are included in the article.

Disclosure

The authors would like to declare that the work described is original research and has not been publicly published previously.

Conflicts of Interest

The authors declare no conflicts of interest.

Authors' Contributions

The work presented herein was carried out in collaboration between all the authors. ZE was responsible for study conception and design. YL was responsible for the data collection. YD was responsible for the analysis and interpretation of the data. All the authors reviewed the results and approved the final version of the manuscript for publication.

Acknowledgments

This study was funded by the Science and Technology Department of the Guangxi Zhuang Autonomous Region, Science and Technology Department of the Guangxi Zhuang Autonomous Region (1598009-11), Research on the Application of Granite Aggregates on the Highway from Guilin to Qinzhou Port (Nanning Liujing to Binyang section) in Guangxi (LBGS-HT-51), and the Department of Science and Technology of the Guangxi Zhuang Autonomous Region (Guike AB20159036). The authors thank LetPub (https://www.letpub.com) for its linguistic assistance during the preparation of this manuscript.

References

[1] J. S. Miller and W. Y. Bellinger, "Distress identification manual for the long-term pavement performance program (5 revised edition)," Report No. FHWA-HRT-13-092, Federal U.S. Department of Transportation Highway Administration, Washington, DC, USA, 2014.

[2] H. Soenen, S. Vansteenkiste, and K. De Maeijer, "Fundamental approaches to predict moisture damage in asphalt mixtures: state-of-the-art review," *Infrastructure*, vol. 5, no. 2, p. 20, 2020.

[3] Aashto T 283-2014, *Standard Method of Test for Resistance of Compacted Hot Mix Asphalt (HMA) to Moisture-Induced Damage*, AASHTO, Washington, DC, USA, 2014.

[4] JTG E20-2011, *Standard Test Methods of Bitumen and Bituminous Mixtures for Highway Engineering*, Ministry of Communications of the People's Republic of China, Beijing, China, 2011, in Chinese.

[5] J Wang-heng, X. N. Zhang, and Z. Li, "Mechanical mechanism of moisture-induced damage of asphalt mixture based on simulation test of dynamic water pressure," *China Journal of Highway and Transport*, vol. 24, no. 4, pp. 21–25, 2011.

[6] R. A. Tarefder, M. T. Weldegiorgis, and M. Ahmad, "Assessment of the effect of pore pressure cycles on moist ure sensitivity of hot mix asphalt using MIST conditioning and dynamic modulus," *Journal of Testing and Evaluation*, vol. 42, no. 6, pp. 1530–1540, Article ID JTE20130095, 2014.

[7] W. Wang, L. Wang, G. Yan, and B. Zhou, "Evaluation on moisture sensitivity of asphalt mixture induced by dynamic pore water pressure," *International Journal of Pavement Research and Technology*, vol. 13, no. 5, pp. 489–496, 2020.

[8] S. Dhakal and R. Ashtiani, "Effect of Different Levels of Moisture Intrusion on the Dynamic Modulus and Tensile Properties of Dense Graded Hot Mix Asphalt Using a Cyclic Moisture Induced Stress Tester," in *Proceedings of the International Conference on Transportation and Development 2016*, Houston, TX, USA, June 2016.

[9] P. Sulejmani, S. Said, S. Agardh, and A. Ahmed, "Moisture sensitivity of asphalt mixtures using cycling pore pressure conditioning," *Transportation Research Record: Journal of the Transportation Research Board*, vol. 2673, no. 2, pp. 294–303, 2019.

[10] R. A. Tarefder and M. Ahmad, "Evaluating the relationship between permeability and moisture damage of asphalt concrete pavements," *Journal of Materials in Civil Engineering*, vol. 27, no. 5, pp. 1–10, Article ID 04014172, 2015.

[11] J. Xie, L. I. Yu-zhi, and L. G. Shao, "Laboratory evaluation on the moisture susceptibility of hot asphalt mixtures by asphalt pavement analyze," *Journal of Hunan University of Science &*

Technology (Natural Science Edition), vol. 20, no. 2, pp. 53–57, 2005, in Chinese.

[12] F. Yin, E. Arambula, R. Lytton, A. E. Martin, and L. G. Cucalon, "Novel method for moisture susceptibility and rutting evaluation using Hamburg wheel tracking test," *Transportation Research Record: Journal of the Transportation Research Board*, vol. 2446, no. 1, pp. 1–7, 2014.

[13] R. P. Izzo and M. Tahmoressi, "Use of the Hamburg wheel-tracking device for evaluating moisture susceptibility of hot-mix asphalt," *Transportation Research Record: Journal of the Transportation Research Board*, vol. 1681, no. 1, pp. 76–85, 1999.

[14] P. Chaturabong and U. Hussain, "The evaluation of relative effect of moisture in Hamburg wheel tracking test," *Construction and Building Materials*, vol. 153, no. 30, pp. 337–345, 2017.

[15] E. M. Twagira and K. J. Jenkins, "Application of MMLS3 in laboratory conditions for moisture damage classification of bitumen stabilised materials," *Road Materials and Pavement Design*, vol. 13, no. 4, pp. 642–659, 2012.

[16] X. Ouyang, C. Zhao, P. Gao, and X. Wang, "Analysis of influencing factors of performance for sandstone asphalt mixture," *IOP Conference Series: Earth and Environmental Science*, IOP Publishing, Bristol, UK, Article ID 012088, 2020.

[17] C. T. Metcalf, W. H. Goetz, Bituminous sandstone mixtures, https://docs.lib.purdue.edu/cgi/viewcontent.cgi?article=2573&context=roadschool.

[18] H. Zhang and H. Li, "Optimization of sandstone concrete pavement materials based on finite element method," *Arabian Journal for Science and Engineering*, vol. 46, no. 11, pp. 10835–10845, 2021.

[19] JTG E42-2005, *Highway Engineering Aggregate Test Regulations*, Ministry of Communications of the People's Republic of China, Beijing, China, 2005, in Chinese.

[20] JTG F40-2004, *Technical Specification for Construction of Highway Asphalt Pavement*, Ministry of Communications of the People's Republic of China, Beijing, China, 2005, in Chinese.

[21] J. B. Metcalf, *NCHRP Synthesis of Highway Practice 235: Application of Full-Scale Accelerated Pavement Testing. TRB*, National Research Council, Washington, DC, USA, 1996.

[22] Mlstestsystems, *MMLS3 Operator's Mannual*, MLS Test Systems Pty Ltd, Stellenbosch, South Africahttps://www.mlstestsystems.com.

[23] Geomedia Research & Development, *SPA Manager Manual*, Geomedia Research & Development, El Paso, TX, USA, 2007.

[24] M. Jurado, N. Gibson, M. Celaya, and S. Nazarian, "Evaluation of asphalt damage and cracking development with seismic pavement analyzer," *Journal of the Transportation Research Board*, vol. 1, no. 2304, pp. 47–54, 2012.

[25] P. He, "Some methods of deleting inordinate values from measuring data," *Aviation Metrology& Measurement Technology*, vol. 15, no. 1, pp. 19-20, 1995.